Smooth vortex precession in superfluid ^{4}He

L. Hough, L. A. K. Donev, and R. J. Zieve
Physics Department, University of California at Davis, Davis, California 95616
(Received 26 April 2001; published 19 December 2001)

We use a vibrating wire to trap circulation in superfluid ^{4}He. When the trapped circulation extends along only part of the wire, continuing as a free vortex through the cell, we can observe the free vortex precessing around the wire. Despite the small vortex core size in superfluid ^{4}He, the vortex motion proceeds in a regular manner, negotiating surface asperities without halting. We attribute this smooth precession to the wire's being substantially displaced from the cylinder's axis. We verify several numerical predictions about the motion, including an asymmetric signature, isolated pinning events, and temperature dependence.

DOI: 10.1103/PhysRevB.65.024511 PACS number(s): 67.40.Vs, 47.32.Cc, 47.37.+q

I. INTRODUCTION

Vortices appear in systems from superconductors and superfluids to weather patterns and blood flow.[1] They underlie complex fluid flows, and motivate computational techniques.[2,3] Measurements of the behavior of one or a few vortices provide test cases for computations and starting points for understanding more complicated vortex systems. Indeed, even small numbers of vortices can produce interesting dynamics, such as the hopscotch motion of two coaxial vortex rings.[4] Yet in classical systems, even *defining* a single vortex can be difficult.[5] For example, in a classical fluid the vorticity fields of two nearby vortices may overlap and resemble a single vortex.

By contrast, a superfluid vortex is well-defined, since circulation is quantized and nonzero vorticity occurs only within the vortex core. In superfluid ^{4}He, the core size is only a few angstroms, and vortices closely approximate the ideal slender vortices of theoretical treatments. Although in principle superfluid experiments can verify theoretical and computational models of vortex dynamics, few measurements can probe individual vortex behavior. Two exceptions are the observation of a precessing vortex in a Bose-Einstein condensate[6] and interference measurements of a superconducting vortex in a thin film.[7] However, these techniques have limitations for dynamical studies, the former because of the condensate lifetime and the latter because of the time for each measurement. Here we discuss a different experiment, which detects single vortex motion in superfluid helium.

Our apparatus consists of a straight wire, stretched inside a cylinder parallel to the axis. A current pulse in a perpendicular magnetic field makes the wire vibrate. The subsequent motion perpendicular to the field is detected as a voltage between the ends of the wire. In the presence of fluid circulating around the wire, the normal modes of the wire's vibration are split, with the beat frequency revealing the circulation around the wire. This technique originated nearly forty years ago in early measurements of quantized circulation in superfluid ^{4}He,[8,9] and was later used to measure circulation in superfluid ^{3}He.[10]

A question that persisted through two decades of vibrating wire measurements is why intermediate circulation values are frequently observed. The expected quantum levels are clearly more stable, but other values occur as well. One suggestion was that a vortex could extend through the fluid from the cell wall to a spot along the wire, then continue as trapped circulation in one direction along the wire. Since only part of the wire supports nonzero circulation, there is only a partial effect on the vibration frequencies, just as for fractional circulation along the entire length of the wire. Recently this idea was verified, originally in superfluid ^{3}He.[11,12] In the geometry described, the free vortex precesses around the wire, driven by the flow field of the trapped circulation. If the wire is displaced from the axis of the cell, the precession results in oscillations of the beat frequency. We will refer to the trapped circulation and adjacent free vortex segment as a ''partially trapped vortex,'' a phrase which emphasizes the connection between them.

Vortex precession was also observed in ^{4}He, with the same cell used for the ^{3}He measurements, although noise in the attachment point motion usually hid any oscillations present.[13] Even the cleanest ^{4}He signal was far more irregular than a typical ^{3}He signature. Furthermore, the earlier generations of vibrating wire measurements in ^{4}He found no recognizable precession signature. One possible explanation of the difference between the ^{4}He and ^{3}He signals is the vortex core radius: 1.3 Å in ^{4}He as opposed to 1000 Å in ^{3}He. The smaller core makes the ^{4}He vortex more sensitive to roughness on the surface of the cell and the wire. Given the difficulty of experiments on rotating superfluid ^{3}He, particularly vibrating wire experiments that must be carried out well below the 2 mK transition temperature, and the appeal of further measurements on a single vortex line undergoing a fundamentally three dimensional motion, we returned to ^{4}He to attempt to resolve a more regular signature there.

Here we report clean vortex precession in ^{4}He. In the process of this work, we have verified several numerical predictions about the details of the motion,[14] which were inspired by the original ^{3}He work.

II. EXPERIMENTAL BACKGROUND

Our experimental setup is similar to that used in previous generations of vibrating wire experiments.[8,9,13] A brass cylinder of height 50 mm and inner radius about 1.5 mm is filled with helium. A NbTi wire a few microns in radius is stretched parallel to the cylinder's axis, entering the cell through Stycast 1266 caps with small holes displaced 0.3 to

0.5 mm from the axis. The wire is glued into the caps with a small weight hanging from it to keep it under tension.

An ideal wire would have doubly degenerate normal modes at its fundamental frequency. However, as explained in detail in Ref. 9, the modes of a real wire are typically nondegenerate, perpendicular, linear modes. The difference in angular frequency $\Delta\omega_0$ probably comes from imperfections in the wire's cross section or mounting. If the wire serves as the core of a superfluid vortex with circulation κ, the normal modes become ellipses with major axes aligned with the original linear modes. The frequency splitting increases to

$$\Delta\omega = \sqrt{(\Delta\omega_0)^2 + \left(\frac{\rho_s \kappa}{\mu}\right)^2}, \tag{1}$$

where ρ_s is the superfluid density and μ is the mass per length of the wire, adjusted for the fluid displaced during vibration. The correction to μ from the superfluid is $\rho_s \pi R_W^2$, with R_W the radius of the wire. An additional correction from the normal fluid is negligible at our temperatures. The lowest nonzero circulation is $\kappa = h/m$, with m the mass of a ^{4}He atom. With $\rho_s = 0.145$ g/cm^3 and $\mu \approx 15 \times 10^{-6}$ g/cm, the angular frequency splitting from this circulation is $\rho_s \kappa/\mu = 9.6$ rad/s.

The magnetic field, about 200 O, comes from two saddle coil magnets. Changing their relative current rotates the field in the plane perpendicular to the wire. For detection purposes, a key point is that in general the wire does not move in a plane perpendicular to the magnetic field. Since the excitation method uses current in the wire and the resulting Lorentz force, the wire always *starts* moving perpendicular to the field; but vibration in this plane usually is not a normal mode. Instead the wire traces out a elaborate path, with its velocity at times nearly or entirely perpendicular to the magnetic field. The induced emf shows beats in the oscillation envelope at frequency $\Delta\omega$. Orienting the field halfway between the two linear normal modes excites the modes equally and leads to complete beats, with or without circulation around the wire.

The voltage signal goes to a 100:1 PAR 1900 transformer at room temperature, then to a Stanford Research Instruments SR560 preamplifier and SR830 lock-in amplifier. The oscillation magnitude is read to the computer through a 16-bit A/D board. In real time, we fit the envelope to an exponentially damped sine wave with four adjustable parameters (amplitude, phase, frequency, and damping). We also save the original digitized decays for possible reanalysis later. The accuracy in ascertaining the beat frequency varies from wire to wire. It depends heavily, for example, on the beat frequency itself. Typically we can extract the beat frequency to 0.1% below 400 mK. The uncertainty arises primarily from mechanical vibrations which shake the wire, rather than from electronic noise.

A partially trapped vortex has less effect on the wire's beat frequency. The beat frequency in this case depends on what part of the wire is covered with the vortex. Since the middle has a larger vibration amplitude than the ends, it contributes more heavily to the final beat frequency. If there is one quantum of circulation on the wire below an attachment point z, and zero circulation above z, then Eq. (1) still holds, with κ replaced by an effective circulation $\langle\kappa\rangle$ defined by[9]

$$\langle\kappa\rangle = \frac{1}{2L}\int_0^z \frac{h}{m}\sin^2\frac{\pi}{L}z'\,dz' = \frac{h}{m}\left(\frac{z}{L} - \frac{1}{2\pi}\sin\frac{2\pi z}{L}\right). \tag{2}$$

Here L is the length of the wire, and we assume that the lowest normal modes are sinusoidal in the z direction.

The conversion from the total beat frequency to the contribution from circulation, Eq. (1), is insensitive at values of $\Delta\omega$ near $\Delta\omega_0$, where the wire's imperfections overwhelm the effect of circulation. The conversion from circulation to attachment point location, Eq. (2), has low sensitivity near both $\langle\kappa\rangle = 0$ and $\langle\kappa\rangle = h/m$. As a result, our measurements are mainly of the vortex moving in the middle of the cell, where our sensitivity lets us locate the attachment point to better than 50 μm.

As mentioned previously, when a vortex is partially attached to the wire, the free portion precesses around the wire, as shown schematically in the inset of Fig. 1. If the wire is displaced from the axis of the cylinder, the length of the free vortex changes as it moves. This would alter the energy in the flow field unless compensated by motion of the attachment point. When the free portion lengthens, the attachment point moves to decrease the length of the trapped circulation. When the free portion reaches its maximum length and begins to get shorter, the attachment point moves in the opposite direction to increase the trapped circulation. We detect the attachment point motion as oscillations in the beat frequency of the wire, with one period corresponding to one circuit of the free vortex segment.

Figure 1 shows the oscillations characteristic of the vortex precession. The two portions of the figure show data taken at different times but with the same cell. Each point represents a separate plucking of the wire. The oscillations correspond

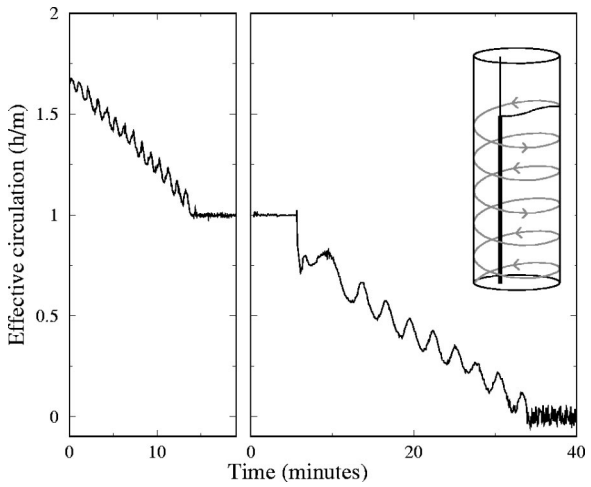

FIG. 1. Trapped circulation decaying through vortex precession. The two parts of the figure have the same horizontal scale. The left portion is at 450 mK, the right side at 330 mK. The inset shows an off-center wire with a vortex partially trapped around it. The free segment of the vortex precesses, with its end point tracing out the indicated spiral.

TABLE I. Estimated dimensions for the five wires used here. R and R_W are the radii of the cell and wire, respectively. ω and $\Delta\omega_0$ are the average angular frequency of the wire's vibration and the splitting between the two lowest modes. T is the precession period of the free portion of a partially attached vortex.

	R (mm)	R_W (μm)	ω (rad/s)	$\Delta\omega_0$ (rad/s)	Smallest T (s)	Predicted T (s)
A	1.4	5.1	6666	25.5	187	138
B	1.4	5.1	4115	3.02		138
C	1.4	8.9	2262	6.53	147	154
D	1.53	8.8	1929	10.3	171	180
E	1.53	8.6	1030	33.8	194	179

to the motion of the free vortex around the wire. The moving vortex dissipates energy. The trapped circulation forms an energy reservoir, with stored energy roughly proportional to its length. Thus the dissipation gradually reduces the length of the trapped vortex, producing the steady circulation decay of Fig. 1. We use the term ''unwinding'' to describe this combination of precession and circulation decay. Figure 1 also shows the qualitative distinction between the expected quantized circulation levels, which we will refer to by quantum number ($n=0$, $n=1$, etc.) and intermediate levels, both at $n>1$ and $n<1$. The quantized levels are far more stable and exhibit none of the oscillations due to precession. The increased noise near $n=0$ is inherent in the analysis equations, as mentioned above. Finally, the figure shows the different precession periods for decays at $n>1$ and $n<1$, roughly 1 and 3 min, respectively. In the former case the circulation around the wire is $2(h/m)$ near one end and h/m near the other, with a singly quantized vortex emerging from the wire at the spot where the circulation changes. The flow field is that of three half vortices, rather than one, so the vortex precesses three times as fast.

We discuss measurements on five wires, which are described in Table I. Each wire is a single strand cut from multistranded NbTi wire. By weighing several strands, and using 6.0 g/cm^3 as the density of NbTi, we find that the average mass per length corresponds to a radius of 5.1 μm for wires such as A and B, and 8.7 μm for wires such as C, D, and E. For the wires that trap a stable $n=1$ vortex, we can take the observed stable beat frequencies as $\Delta\omega$ and $\Delta\omega_0$ in Eq. (1) and find the mass per length of the wire. The corresponding radius values, shown in Table I, are close to the values found from the weights. For wires A and B, no stable $n=1$ state was seen, and Table I shows the radius calculated from the typical wire weight. As an additional check, the room temperature resistance of the wires should be proportional to cross-sectional area. The radius values in Table I are indeed consistent with the wires' resistances. As discussed below, the amplitude and shape of the oscillation signals depend on the displacement from the cylinder axis. Our observations are consistent with the displacements measured during assembly of the cells.

The measurements are performed on a pumped ^{3}He cryostat with a minimum temperature of 250 mK. The cryostat has an external ^{4}He pumping line, which passes through a rotating vacuum seal. For the experiments discussed here, all measurements are made with the cryostat stationary. We fill the cell at 4 K, then cool into the superfluid phase. Once cold, we rotate by hand, typically ten revolutions in one minute, to create circulation. During rotation our electrical wires are disconnected. When we restart the measurements, we usually find an unstable state, which can have circulation either larger or smaller than the $n=1$ state. If the circulation settles to a stable $n=1$ state, we dislodge the vortex by moving the cryostat rapidly about 60°, in the direction opposite to the previous rotation direction, and then slowly returning it to its original position. This minimally controlled shaking generally results in one of two vortex signatures. Sometimes an abrupt drop in trapped circulation is followed by oscillations indicating vortex precession. At other times, the circulation drops, but then increases back to $n=1$ in the characteristic, slightly irregular way illustrated several times in Fig. 2. One possible explanation is that a portion of the vortex is dislodged from the wire, but does not reach the cell wall. The detached portion then precesses around the wire, spiraling inward until it is recaptured by the wire. The detaching could occur near the center or end of the wire; schematics of these two possibilities are shown in Fig. 2.

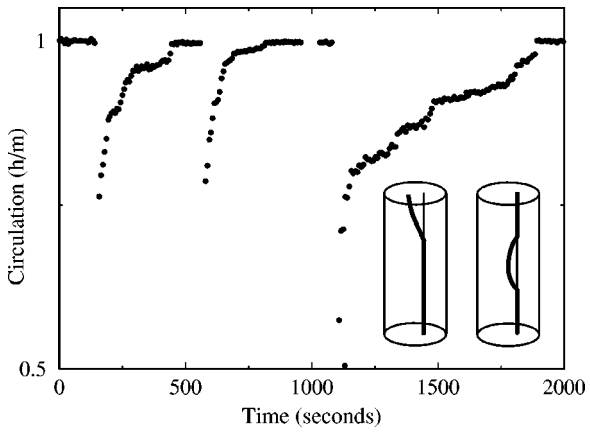

FIG. 2. Characteristic signal for vortex partly dislodging and returning to wire, at 340 mK. The insets show two possibilities for the vortex configuration corresponding to the intermediate circulation values.

III. COMPUTATIONAL BACKGROUND

To complement our experimental work, we do simulations of superfluid vortex dynamics. A numerical rather than analytic approach is required because the off-center wire destroys the problem's cylindrical symmetry. Our code is similar to that of Schwarz,[14,15] and is described elsewhere.[16] Here we briefly summarize its workings. The equations of motion for the vortex are based on the incompressible Euler equations, which by themselves would require the vortex core to move at exactly the local superfluid velocity. A friction term $-\alpha\mathbf{s}'\times\mathbf{v_s}$ is added which gives the vortex motion an additional component perpendicular to the superfluid velocity. Here the friction coefficient α determines the strength of the friction interaction; $\mathbf{s}'$ is the tangent to the vortex line, directed so that the circulation is given from $\mathbf{s}'$ by the right-

hand rule; and $\mathbf{v_s}$ is the superfluid velocity. We calculate the fluid velocity from the instantaneous core locations and boundary conditions imposed by the cylindrical container. The vortex cores have a local contribution proportional to the vortex curvature, and a nonlocal contribution from distant segments which obeys the Biot-Savart law. For the present geometry, we neglect the latter except for the portion of the vortex trapped along the wire, which we treat as a semi-infinite straight vortex. We meet the boundary conditions approximately using an image vortex: a second semi-infinite vortex defined from the trapped vortex by inversion in the cylinder. Adding images of the free vortex segment, under inversion in the cylinder or wire, does not significantly change the results.

Sonin[17] has argued that the nonlocal contribution from the trapped circulation and the local contribution from the free portion partly duplicate each other, leading to inaccuracies in the free vortex shape. The magnitude of the discrepancies is of order

$$\frac{\ln\frac{R}{R_W}}{\ln\frac{R}{a_0}}, \tag{3}$$

where R, R_W, and a_0 are the radii of the cell, wire, and free vortex core, respectively. The small core size in ^{4}He as opposed to ^{3}He reduces this quantity, bringing the two approaches closer together. For the semi-quantitative results presented here, either approach should suffice. If Sonin's objections prove to be correct, we expect minor corrections to our calculations.

We use dimensions similar to those of the actual experiment: a cell of radius 1.5 mm, and a wire of radius 6 μm. Near the wire the point spacing along the vortex is comparable to the wire radius, and it gradually increases with increasing distance from the wire.

IV. SMOOTH PRECESSION

In the absence of dissipation, the precession period for a single partially attached vortex is given by[11]

$$T=\frac{4\pi^2(R^2-R_W^2)}{\kappa\ln\frac{R}{R_W}}. \tag{4}$$

Published derivations include a discussion of forces,[11] an interpretation as a macroscopic Josephson effect,[18] and both analytic[14,17] and computational[14] treatments of the superfluid hydrodynamics equations. As shown in Table I, the predicted and actual values for our cells are in reasonable agreement, with typical precession periods slightly under three minutes. The discrepancies are larger than in ^{3}He,[11,12] or in lower-temperature ^{4}He[13] measurements. A major reason for this is that in our temperature range the precession period varies substantially with temperature. We discuss this behavior below.

We first address the smooth nature of the motion, not previously found in ^{4}He. For four of the five wires, the oscillations indicating vortex precession are clearly visible and quite regular. For the fifth, wire B, circulation decays rapidly with no clean precession. These are the *only* wires that we have measured, so the contrast with the noisy intermediate-circulation data from the previous experiments is striking. The one deliberate difference in our design is that, instead of trying to center the wire in the cylinder, we intentionally move it off the axis to increase the amplitude of the precession oscillations. We suggest that a displaced wire also leads to smoother vortex motion.

We use a critical angle model[15] for calculating the interaction of the precessing vortex with the cylinder wall. We incorporate pinning without any geometrical details of the pin sites; rather, we simply fix the position of one end of the vortex at a spot on the cylinder wall. The local fluid velocity bends the vortex towards the wall. If the angle between the vortex and the wall normal exceeds a critical value, the fixed end of the vortex becomes free to move along the cylinder wall. If the critical angle is too large, the vortex never reaches it and remains pinned. Physically the critical angle represents the scale of the wall roughness, with larger critical angles corresponding to sharper protuberances. For a simulated vortex to precess without becoming permanently pinned, the angle must be sufficiently small. Here we examine how the position of the wire affects the possible values of the critical angle.

We begin by finding the trajectory of a precessing vortex. Initially, waves propagate along the vortex as it settles into the configuration appropriate for steady precession. Once these oscillations in the vortex shape have decayed away, we pin the end of the vortex. The vortex again oscillates, settling gradually into a permanent position. We find the maximum angle with the wall normal achieved during this process, shown in Fig. 3 for an on-center wire and for one displaced 0.4 mm. We have previously shown that prescribing pinning externally gives nearly identical results to letting a vortex interact with a bump on the cell wall, with the appropriate bump size determined by the point spacing along the vortex.[16] For the present calculations the point spacing near the wall is 53 μm, corresponding to a hemispherical bump of radius 23 μm. As the wire becomes farther off center, the maximum angle increases substantially at most locations in the cell, but decreases slightly where the vortex is longest.

In the calculations for Fig. 3 we do not allow the vortex to depin. If we did, depinning would occur for any critical angle smaller than the maximum vortex-wall normal angle. In most of the cell, the off-center wire allows depinning with larger critical angles. Schwarz[14] also finds that an off-center wire and a pin site near $\theta=75°$ support depinning at larger critical angles than an on-center wire. However, Fig. 3 suggests that near 180° the off-center wire actually makes depinning more difficult. From this we might expect an off-center wire to lead to smoother vortex motion in most of the cell, but to increased disruption from pinning near 180°. Experimentally we find regular precession signals throughout the cell, so further explanation is required.

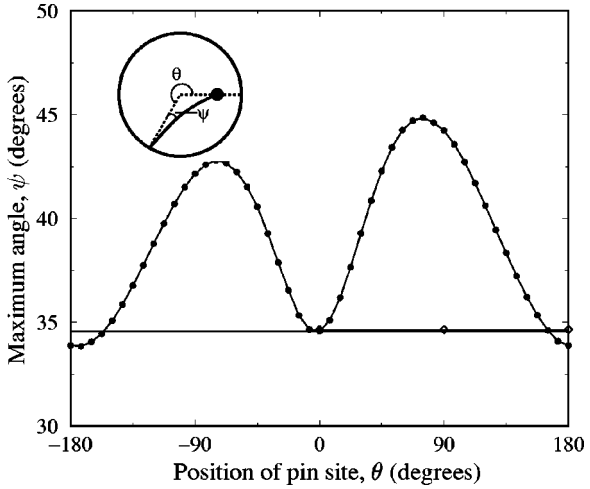

FIG. 3. Maximum angle from wall normal that occurs as vortex settles into pin site, obtained by simulation. The calculations use no friction ($\alpha=0$). ◇: wire on cylinder axis. ●: wire displaced 0.4 mm from cylinder axis. The inset shows the geometry. The black dot represents the wire, which has counterclockwise circulation on the portion away from the viewer. The thick solid arc is the free segment of the vortex. The angle ψ may lie out of the plane of the page.

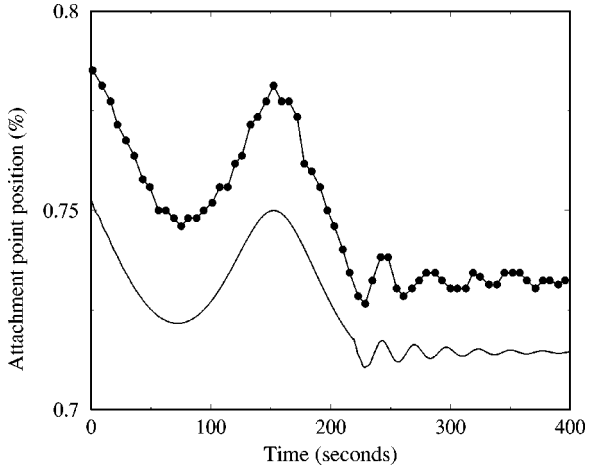

FIG. 4. Vortex becoming pinned during its precession. Top curve: measurements at 345 mK. Bottom curve: simulation for wire displaced 0.25 mm from cell center, pin site at $\theta=126°$, friction coefficient $\alpha=0.05$.

One possibility is that the wall roughness involves irregularities of different sizes, each with its own critical angle. Places which pin vortices more easily correspond to larger critical angles. As long as the most effective pin sites lie outside the narrow region near 180° with enhanced pinning for the off-center wire, moving the wire off center may still reduce pinning.

Another issue is that the configuration at the onset of a pinning event affects the maximum angle achieved. We use precession in a perfectly smooth-walled cell to define the vortex shape just before encountering a pin site. This approach is reasonable if wall irregularities are far enough apart. On the other hand, just after coming free from a bump a vortex line has a different shape, bent closer to the cell wall. With enough wall roughness the vortex would not have time to relax to its smooth-cell configuration between bumps, and the initial shape we use may be a poor approximation.

The main influence on the allowed critical angle comes from the cell geometry. Given a free vortex segment with one endpoint on the wire and the other on the cylinder wall, the straight line connecting the endpoints is a first approximation to the shape of the vortex. For an off-center wire, the line is only perpendicular to the cell wall at $\theta=0°$ or $\theta=180°$. The line's largest deviations from perpendicular occur near the maxima of Fig. 3. Although the actual vortex deviates from the straight line, an energy associated with bending limits the distortion.

The fluid velocity field has a lesser effect on critical angles. The velocity is faster than for an on-center wire where the wire approaches the cell wall closely (θ near 0°), and slower where the wire-wall distance is larger (θ near 180°). The reduced velocity field causes the slightly lower maximum angle at 180° relative to 0°. The velocity field, through its direction relative to the vortex curvature, also produces the asymmetry between the two sides of the cell.

Apart from the displaced wire, nothing about our setup differs substantially from two previous sets of experiments at temperatures below 400 mK.[13,19] Our cylindrical cells have comparable dimensions to those in the earlier work. They are drilled or reamed, with no special polishing or other treatments, so the cell walls are probably no smoother than in the earlier experiments. Although our wires are the smallest used to date, our larger wires are within a factor of 2 of nearly all those previously reported. We believe that a smaller wire size improves the precession signatures only in a minor and indirect way. Most of our measurements are on vortex precession between $n=1$ and $n=0$, although we also observe precession between $n=2$ and $n=1$, as shown in Fig. 1. In previous experiments slow transitions were usually found only between the higher circulation levels, with $n=1$ so stable that only steadily rotating the cryostat in the opposite sense to the vortex would dislodge it. From Fig. 1, the $n=2$ to $n=1$ precession may be slightly noisier than that from $n=1$ to $n=0$, but it is clearly visible and far cleaner than previous ^{4}He precession data.[13] The lower-circulation motion may be more regular because less vorticity remains in the cell. If so, our smaller wires smooth the precession signature by favoring precession at $n<1$, but are not a crucial feature of the current experiment.

V. PINNING

Figure 4 shows the signature computed for pinning of the vortex line by the cell wall, along with an experimental signal that we attribute to pinning. The precession oscillations at the left give way to faster, lower amplitude oscillations upon pinning. The energy dissipation leading to the decay of the trapped circulation also ceases, as expected once the vortex stops moving. Schwarz's simulations show analogous signatures for depinning events,[14] but experimentally the onset of pinning is easier to study. After pinning, with no precession

or dissipation, the background circulation level is conveniently constant. By contrast, any signature from depinning is superimposed on both the oscillations from vortex precession and the linear change from decay of the trapped vorticity. In addition, if an external perturbation causes the depinning, other irregularities may occur in the decay signal just after the event.

The fast oscillations upon pinning seen in Fig. 4 arise from Kelvin waves on the free vortex segment. Kelvin originally treated vortex waves on an infinite vortex, straight except for a sinusoidal distortion of wave number k.[20] The distortion rotates about the average core position at frequency $\omega = \kappa k^2 A/4\pi$. Here $A \approx \ln(1/ka)$ and a is the core radius. The boundary conditions of our experimental setup require a standing wave, which can be obtained by combining waves rotating in opposite directions. With a node on the cell wall and maximum displacement on the wire, we require $k = \pi/2d$ for the lowest mode, with d the distance from the wire to the pin site.

In the experimental data of Fig. 4, the free vortex segment is longest at 75 sec, since the attachment point position has a minimum there. The pinning occurs near 223 sec, or about 85% of one period after the free vortex is at its longest. From the amplitude of the precession oscillations, the estimated wire displacement is 0.25 mm. Then the distance from the wire to the pin site is 1.7 mm. The corresponding straight vortex mode has $\omega = 0.11$ rad/s and period 58 sec, substantially longer than the observed period of 37 sec. The discrepancy comes largely from the effect of the cylindrical container, which changes the equilibrium configuration by forcing the vortex to bend. The vortex line tension, or how the energy changes with length, depends strongly on configuration. Indeed, even in a parallel-plane geometry, vortex curvature can significantly change the Kelvin oscillation period.[16]

Pinning simulations for the present experimental geometry confirm the period change. As described in the previous section, we begin with a steadily precessing vortex and suddenly fix its end at the wall. We choose the pin location to match the measured pin event. We note that, in keeping with our critical angle simulations, the pin site in Fig. 4 is near where the free vortex is longest (i.e., $\theta = 180°$ in Fig. 3). This is also true for the other long pinning events we observe. The simulations show oscillation of the free portion, coupled to motion of the attachment point up and down the wire, with period 29 sec. The discrepancy between the simulation and experiment may come from our uncertain knowledge of the wire's displacement and the pin site's location in the cell. Our data are the clearest observations to date of Kelvin waves on a single superfluid vortex line.

The damping of the Kelvin mode is many orders of magnitude too high to come from mutual friction with the normal fluid. Since one end of the free portion of the vortex is stationary at the wall, it is likely that the dissipation comes from the other end as it moves up and down along the wire.

VI. ASYMMETRIC OSCILLATIONS

Another feature predicted by Schwarz[14] is a slight asymmetry in the precession signature. The vortex velocity depends on the local fluid velocity. If the wire were centered in the cylinder, the fluid velocity would have no angular dependence. With the off-center wire, boundary effects increase the velocity where the wire is closest to the wall, so the vortex moves more quickly on this side. In the precession signal, the fastest motion occurs at the top of each cycle, when the free vortex is short. The slowest precession is at the lowest trapped circulation, when the free vortex is longest. The result is slightly sharpened peaks and rounded troughs.

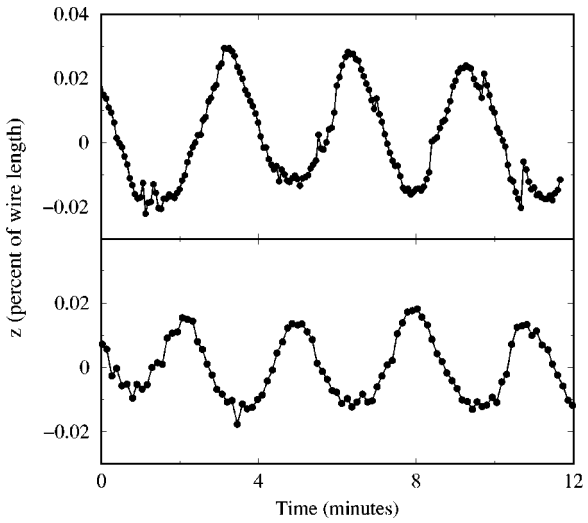

FIG. 5. Asymmetry in the precession oscillations, for wires A (upper) at 380 mK and C (lower) at 335 mK. Note the relative roundedness of the troughs and sharpness of the peaks.

Figure 5 shows exactly this structure, for wires A and C. To remove the overall slope caused by energy loss, a line has been subtracted from each data set. Both the oscillation amplitude and the asymmetry are larger for wire A than for wire C, implying that wire A is farther off center. Our observation of the asymmetry in the precession signal is encouraging for the eventual goal of being able to track more complicated motion of a single vortex.

VII. TEMPERATURE DEPENDENCE

Another of Schwarz's predictions involves temperature dependence.[14] In addition to its interaction with the local velocity field, a vortex line feels a frictionlike force proportional to its velocity relative to the stationary normal fluid. The friction force determines the energy loss, and hence the linear decrease of circulation with time that appears along with vortex precession. Experimentally, the friction coefficient α depends strongly on temperature. Figure 6 illustrates the dramatic change in energy loss rate upon changing the temperature from 340 to 380 mK.

Computer simulations reveal that with increased α the vortex not only moves downward more rapidly, but also precesses less quickly.[14] We now find experimentally that, as temperature increases, the dissipation rate and the precession period also increase. While the period change is small—only 6% in Fig. 6—it is certainly outside our measurement error.

One difference between the simulations and experiments is the source of the friction. In the simulations, the dissipa-

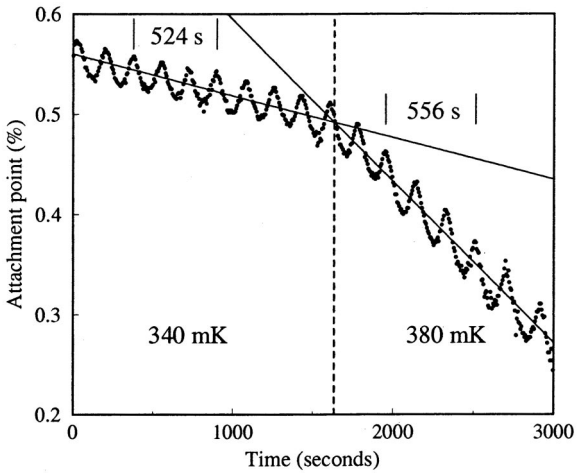

FIG. 6. Dependence of precession rate and dissipation on temperature. The solid lines are guides to the eye. The times for three periods are indicated, with the period increasing a small but noticeable amount with temperature.

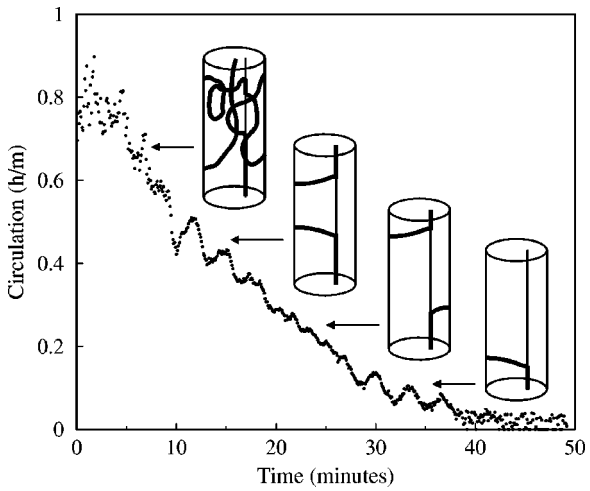

FIG. 8. Vortices unwinding from both ends of the wire simultaneously. The schematics illustrate possible vortex configurations at the times indicated. Temperature is 320 mK.

tion comes from mutual friction, the interaction between the vortex and the normal fluid. This is not the case in experiments. In our temperature range, mutual friction is many orders of magnitude too small to account for the observed dissipation.[21] As with the damping of Kelvin waves along the free vortex, the most likely dissipation mechanism is the rubbing of the end of the vortex along the wall and wire. It is interesting that the relationship between the precession rate and the dissipation holds nonetheless.

In the limiting case of large dissipation, Schwarz finds that the vortex moves directly downward without precessing at all.[14] Our wire B has this behavior; its circulation decay is very fast and exhibits no oscillations.

VIII. INITIATING PRECESSION

In the work described here we usually shake the cryostat to initiate the vortex motion. However, in superfluid ^{3}He (Ref. 12) and occasionally in our present measurements, a trapped vortex may leave the wire without deliberate external perturbation. How the unwinding process begins remains unknown. Schwarz suggests that a free vortex in the cell collides with the $n=1$ vortex along the wire.[14] Close approach of vortices often leads to a runaway attraction ending in reconnection,[15] illustrated in Fig. 7. The vortices are cut at the crossing point, and the segments leading in and out are reattached in the opposite way. A reconnection involving one free vortex and one trapped around the wire might create two partially attached vortices.

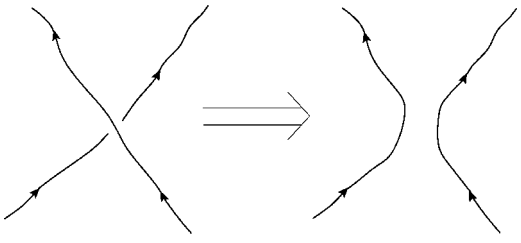

FIG. 7. Vortices reconnecting upon collision.

Figure 8 shows what we believe to be two unwinding partial vortices. The cryostat was rotated immediately before the data pictured. From the irregular circulation signal for the first few minutes we hypothesize that a jumble of vortices pervades the cell. After 10 min precession begins, with the usual period near three minutes and large amplitude oscillations. This behavior is consistent with two partially attached vortices, which are on the same side of the wire at the same time. Additional structure appears in the decay, and by 20 min the frequency has doubled, with the amplitude dropping dramatically. One explanation is that the two precessing vortices are now out of phase. If one is long while the other is short, their effects on the trapped vortex length partly cancel, reducing the oscillation amplitude. (The cancellation cannot be complete. Since the superfluid velocity field, and hence the precession rate, depend on the position within the cell, the two vortices cannot remain perfectly out of phase with each other.) The frequency doubling occurs because the two vortices attain an equivalent configuration, with their roles transposed, after each traverses only half of the cell. Finally, after 30 min, the oscillations return to the usual precession frequency. These are cleaner than the large oscillations earlier in the decay, and signify that one of the vortices has completed its unwinding, returning the cell to a single-vortex situation.

We have calculated numerically the energy in the flow field for two partially attached vortices if they are on the same or opposite sides of the cell. The out-of-phase configuration is energetically favorable, which is consistent with its appearance in our observations. We have not yet investigated how the vortices change from in-phase to out-of-phase. We have seen one other signature similar to that of Fig. 8. Since the more common vortex precession signatures, as in Figs. 1 and 6, are much cleaner, we believe that they involve only one partially attached vortex. This means that the unwinding

process generally does *not* start from a collision with a free vortex, since even unwinding that begins without shaking rarely leads to signatures similar to that of Fig. 8.

IX. CONCLUSIONS

We have presented data on smooth vortex precession in superfluid ^{4}He. A key difference between our work and other vibrating wire measurements is that our wires are located substantially away from the axis of the container. We verify several numerical predictions for precession signatures: behavior at pinning events, the oscillation asymmetry from the off-center wire, and the relationship between the vertical motion of the trapped vortex and its precession period. The repeatable, smooth vortex precession can serve as a probe in further experiments on dynamics of one or a few vortices.

Our measurements also address the question of how the precession begins. We see a distinctive signature for two partially attached vortices. Its absence in the bulk of our measurements means that this configuration rarely initiates the precession. A more common situation appears to be a partially dislodged vortex which may return to the wire or change to terminate on the cell wall. Since many of our vortex decays begin with literally shaking the cryostat, our typical detachment mechanism may differ from behavior in the absence of such strong external perturbations. Better controlled studies of how the vortex first comes off the wire remain to be done.

[1] H.J. Lugt, *Vortex Flow in Nature and Technology* (John Wiley & Sons, New York, 1983).

[2] L. Ying and P. Zhang, *Vortex Methods* (Science Press, Beijing, 1997).

[3] S.M. Belotserkovskii and I.K. Lifanov, *Method of Discrete Vortices* (CRC Press, Boca Raton, 1993).

[4] H. Yamade and T. Matsui, Phys. Fluids **22**, 1245 (1979).

[5] S.I. Green, *Fluid Vortices* (Kluwer Academic Publishers, Dordrecht, 1995), Chap. 1.

[6] B.P. Anderson, P.C. Haljan, C.E. Wieman, and E.A. Cornell, Phys. Rev. Lett. **85**, 2857 (2000).

[7] M. Breitwisch and D.K. Finnemore, Phys. Rev. B **62**, 671 (2000), and references therein.

[8] W.F. Vinen, Proc. R. Soc. London, Ser. A **260**, 218 (1961).

[9] S.C. Whitmore and W. Zimmermann, Jr., Phys. Rev. **166**, 181 (1968).

[10] J.C. Davis, J.D. Close, R. Zieve, and R.E. Packard, Phys. Rev. Lett. **66**, 329 (1991).

[11] R.J. Zieve *et al.*, Phys. Rev. Lett. **68**, 1327 (1992).

[12] R.J. Zieve *et al.*, J. Low Temp. Phys. **91**, 315 (1993).

[13] R.J. Zieve, J.D. Close, J.C. Davis, and R.E. Packard, J. Low Temp. Phys. **90**, 243 (1993).

[14] K.W. Schwarz, Phys. Rev. B **47**, 12 030 (1993).

[15] K.W. Schwarz, Phys. Rev. B **31**, 5782 (1985).

[16] R.J. Zieve and L.A.K. Donev, J. Low Temp. Phys. **121**, 199 (2000).

[17] E.B. Sonin, J. Low Temp. Phys. **97**, 145 (1994).

[18] T.S. Misirpashaev and G.E. Volovik, JETP Lett. **56**, 41 (1992).

[19] P.W. Karn, D.R. Starks, and W. Zimmermann, Jr., Phys. Rev. B **21**, 1797 (1980).

[20] W. Thomson, Philos. Mag. **10**, 155 (1880).

[21] G.W. Rayfield and F. Reif, Phys. Rev. **136**, A1194 (1964).